Laboratory Scale Study of Reverse Priming in Aluminium Filtration

Sarina Bao[1], Martin Syvertsen[1], Freddy Syvertsen[2] Britt Elin Gihleengen[3], Ulf Tundal[4], Tanja Pettersen[1]
[1]SINTEF Industry, Alfred Getz Vei 2B, 7034 Trondheim, Norway
[2] Syvertsen Støperikonsult, Tonstadgrenda 13, 7091 Tiller, Norway
[3]Hycast AS, Industriveien 49, 6600 Sunndalsøra, Norway
[4]Hydro Aluminium, Romsdalsveien 1, 6600 Sunndalsøra, Norway
Corresponding author: Tanja Pettersen, Alfred Getz vei 2B, NO-7034 Trondheim, Norway
e-mail: tanja.pettersen@sintef.no

Keywords: Reverse priming, Priming, Aluminium, Filtration, Ceramic foam filter

Abstract

Inclusions are one of the most serious problems encountered in aluminium production and melt treatment. Even small inclusions, not larger than a few tens of micrometres, can potentially have considerable consequences for the down-stream processing and a detrimental effect on the final product.

Ceramic Foam Filters (CFFs) are commonly used to remove inclusions from the melt before the casting process. The very first phase of the filtration is called the priming period. This is when the molten metal meets the filter and fills up the pores inside the filter. In order to obtain good priming and to avoid freezing of the metal inside the filter, the filter must be properly preheated.

During standard operation in industry, the metal flow direction during priming is typically the same as the metal flow during filtration. In the present work, equipment for testing the effect of reverse priming has been developed. Tests with standard and reversed priming directions have been carried out and the spent filters have been examined. The interface between the metal and the filter has been studied and it is concluded that all filters were well primed no matter the priming direction.

Introduction

In the past few decades, CFF is known as one of the most popular ways to remove inclusions from aluminium before casting [1-10]. Hycast has recently filed a patent for a new filter box [11], which, somewhat simplified, can be said to be a hybrid of a conventional filter box and the Hycast Siphon Inert Reactor (SIR) unit [12]. In addition to the self-emptying filter box, one of the main innovations is how the priming of the filter is done. The metal flows in from below and the filter will be primed from the bottom. Once the filter is primed, the metal flow is reversed, and filtration is done with metal flowing from top to bottom for the rest of the cast.

Aluminium is always covered with an oxide film. The theoretical equilibrium limit of oxygen partial pressure for formation of Al_2O_3 is 10^{-49} bar [13] at 700 °C (10^{-49} bar corresponds to far less than one O_2 molecule in the whole of earth's atmosphere.). When aluminium primes the filter, the metal is filled into a smaller area, and the films will fold and entrain into the melt or tear under the tension at the thinnest point, as described by John Campbell [14]. With reversed priming, the interface between the metal and filter can be different than without reversed priming. In both cases, bulk turbulence may tear oxide films away from the liquid metal surface and transport them towards the filter interface.

In the present study we investigate in lab-scale if the direction of priming influences the priming and filtration behaviour and, in particular, the metal and filter interface.

Experimental Procedure

An experimental set-up was built which enabled priming followed by filtration in the reversed direction, in addition to standard priming and filtration. 150 kg of pure Al (Al 99.88, Si 0.06, Fe 0.06, Ca 0.01, Ti 0.01, V 0.01, other <0.01 wt.%) was melted in a Low-Pressure Die-Cast (LPDC) furnace as shown in Figure 1. The metal was heated up to 750 °C and held at this temperature during the period of the test campaign. Two sand moulds, made by SINTEF, were mounted together with a $10\times10\times5cm^3$ 50 ppi alumina filter (88 wt% Al_2O_3 and approximately 10 wt%, P_2O_5-information from Pyrotek Scandinavia) in-between as shown in Figure 2. The filters were preheated at 800 °C. The metal was pushed up and through the preheated riser tube by using Ar with controlled flow rate. To stop the metal flow, the paddle (in a form of a steel plate) was closed with a hammer. To simulate priming and filtration, the metal was pushed up until the filter was primed and we observed some metal in the top container, then flushing of Ar was stopped, and the metal went down through the filter again without emptying the container completely. In the last trial, pressed kitchen foil of 1391 g was melted in with the same Al ingot (40 wt% foil addition) and induced into the furnace (Figure 3). This melt was then poured into the filter from the top, with the intention of studying the inclusion removal ability of the filter after reverse priming. Samples were taken from the induction furnace for microstructure analysis.

The gas pressure (P_{Ar}, Figure 1 to the right) was measured on the gas line between the Alicat MFC (Mass Flow Controller) and the pressure chamber inside the pump. The furnace melt temperature, temperature below the filter, and gas flow, and gas pressure inside the pump were logged during the test. The filter mass before and after the test was also recorded. The spent filter (Figure 3) was cut diagonally and examined in light microscopy.

Nikon XT 225S 3D Micro x-ray computed tomography analysis was carried out to explore the overall infiltration behaviour in the spent filter.

Hence, 3 groups of tests were performed: (1) upstream with pure Al, (2) up-and-down stream with pure Al, and (3) up-and-down stream with oxide films incubated Al melt.

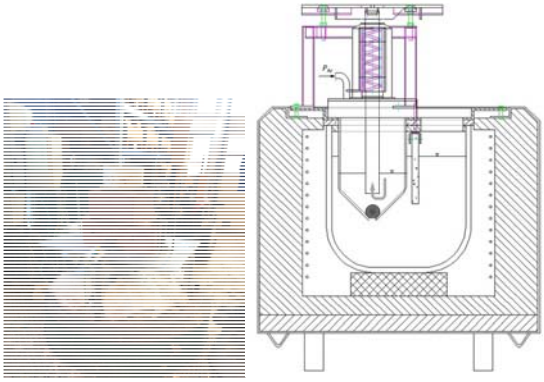

Figure 1 The experimental set up (left) and the sketch of melting furnace and metal lifting system (right)

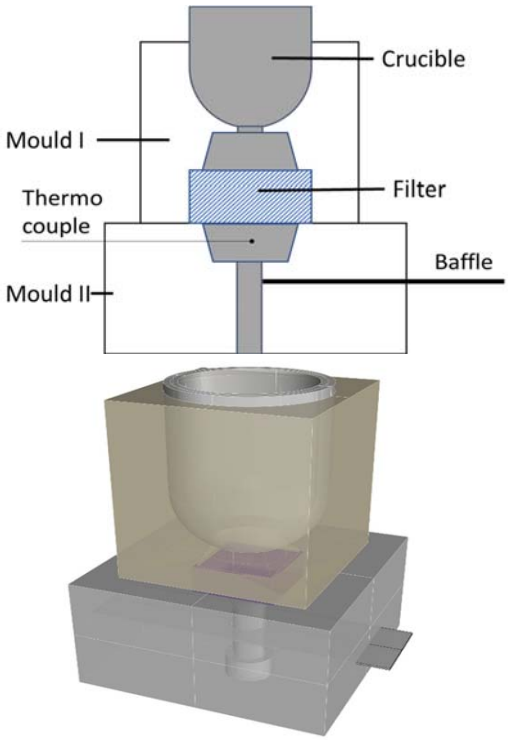

Figure 2 The sketch of two sand moulds and filter in the middle (cross section and 3D)

Figure 3 The cross section of the sand mould after test (left) and pressed Al kitchen foil for melting (right)

Results and Discussion

Some work was done to adapt and test the set-up. It was confirmed that the argon gas pumping system together with sand moulds works well with respect to the purpose of this work. No leakage of metal was observed during the tests and the metal ran through the filter as expected. The metal was pushed upwards through the filter by adjusting the gas flow stepwise up to 14 normal L/min. Due to the difficulty of monitoring the exact moment when the metal flow changed direction, in addition to the force that was needed to hammer in the paddle, it was difficult to stop the metal flow at the right moment. Hence, several trials were carried out to obtain the 3 tested conditions. The logging system worked well, as shown in Figure 5 to Figure 8. Four tests, as shown in Table **I**, will be discussed here. The average spent filter weight is (1260 ± 40) g, which gives 530 % weight gain during the test. The filter weight before test was (200 ± 6) g out of 5 pieces.

Table I Experimental overview

Test	1	2	3	4
Remarks	Up/ down	Up/ down	Up	Up/down +Al foil
Spent filter weight in g	1318	1266	1194	1274
Average pressure increase under the filter in mbar/min	38	71	72	108
Estimate of flow rate in mm/s	2.7	5.1	5.2	7.8
Estimate of flow rate in kg/(min·m^2)	392	732	742	1113
Estimate of the flow rate in 10×10 cm^2 filter in kg/min	4	7	7	11
Corresponding flow rate in 20×20 inch^2 filter in kg/min	101	189	191	287

The flow (lifting) rate of the metal was calculated, and is displayed in Figure 4, with gas flushing up to 8 normal L/min. The measured pressure drop can be defined as

$$\frac{\Delta P}{\Delta t} = \rho g \frac{\Delta h}{\Delta t} = \rho g v \quad (1)$$

where ΔP is the pressure increase, ρ is the liquid density of 2375 kg/m^3 for pure molten Al, g is the acceleration of gravity, 9.8 m/s^2 and Δh is the height or moving distance of the liquid, Δt is the time interval, and v is the velocity of the liquid.

Using Si-units:

$$\frac{\Delta P}{\Delta t} = 112 \frac{mbar}{min} = 187 \frac{Pa}{s} \quad (2)$$

which gives:

$$v = \frac{187\,\frac{Pa}{s}}{2375\,\frac{kg}{m^3}\cdot 9.81\frac{m}{s^2}} = 8.1\frac{mm}{s} \quad (3)$$

Neglecting resistance to flow and by assuming negligible pressure drop through the filter we can derive a linear metal velocity as function of pressure increase of:

$$v\left(\frac{mm}{s}\right) = \frac{\frac{\Delta P}{\Delta t}\left(\frac{mbar}{min}\right)}{13.83} \quad (4)$$

which can be used to give a first estimate of the metal flow velocity through the filter in the tests, at least in upwards direction.

The flow rate of the 4 tests is calculated according to the measured pressure increase as shown in Figure 4 and presented in the 3rd row in Table **I**. The area flow rate regarding 10 cm square for this work and 20 inch square industrial sized filter is calculated and displayed in the last 2 rows. As recommended from the supplier of SIVEX filters, the suggested flow rate of a 20 inch filter is 333 kg/min. This indicates that our results are within the same range, but they show lower flow rate.

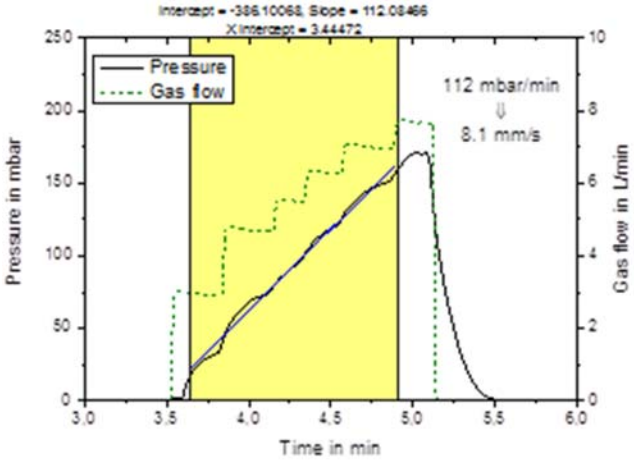

Figure 4 The pressure and gas flow during the lifting test (the yellow area represents the values used for calculating the slope/average pressure increase)

As shown in Figure 5 for Test 1, the metal (734 °C) filled up the riser with flow rates from 5.0 L/min to 9.2 L/min, until it started to prime the preheated filter. The priming started with a pressure of 196 mbar in the lifting system, until the up-stream metal dropped down again due to the gravity at 14 L/min gas flow with built up pressure of 271 mbar. The filter temperature increased from 660 °C (at the beginning of priming) to 716 °C (up flow) during test. Just after start of the down flow, the gas flushing was stopped, and the sand mould was removed from the set-up. The spent filter was then allowed to cool by natural cooling.

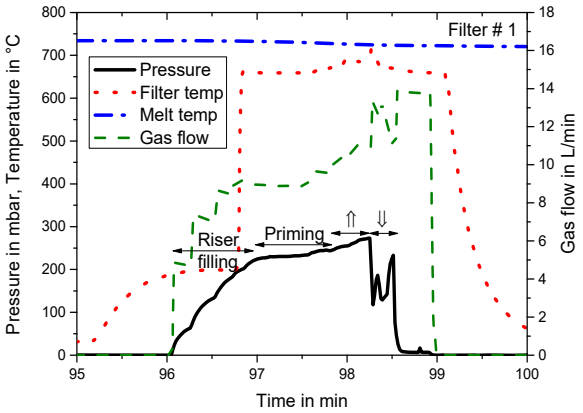

Figure 5 The pressure, gas flow, and temperature during test 1

Similarly, as shown in Figure 6 for test 2, the metal with 733 °C has primed the preheated filter with pressure from 193 mbar (10L/min gas flow) to 256 mbar (14L/min), until the metal flowed down again. The pressure dip at approximately 238.5 min shows the effect of stopping the metal by the paddle.

Similarly, the preheated filter was primed with metal from pressure 186 mbar (10 L/min) to 245 mbar, then the metal run upward until 266 mbar (13 L/min), when the paddle was closed, as shown in Figure 7 for test 3. The metal only run upward until it solidified inside the filter in this test.

The temperature log in test 4 was not successful, as shown in Figure 8. The metal started to reverse prime the filter from 194 mbar (10 L/min) to max. 255 mbar pressure. The dips of pressure drop were related to the feeding of metal from the top.

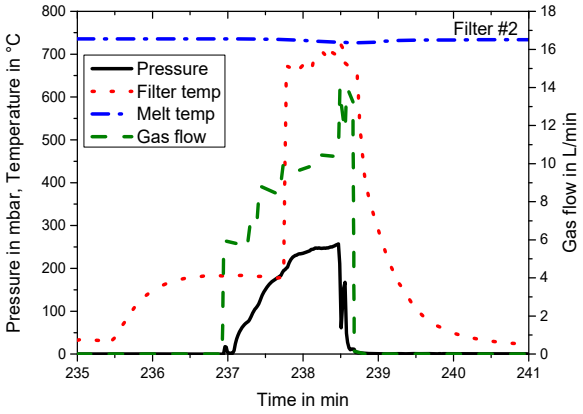

Figure 6 The pressure, gas flow, and temperature during test 2

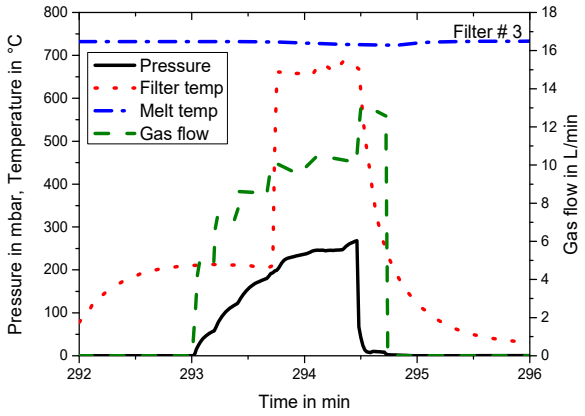

Figure 7 The pressure, gas flow, and temperature during test 3

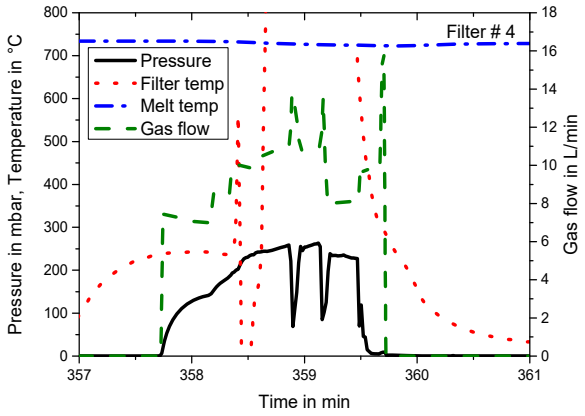

Figure 8 The pressure, gas flow, and temperature during test 4

Figure 9 shows the diagonal cross section view of the spent filter. In general, the metal seems to infiltrate the whole filter, no matter the flow direction and with or without inclusion incubation. The addition of inclusions is done after priming and is not expected to influence the infiltration. However, some unfiltered areas and pores have been seen in all four tests, especially in test 3 and test 4. But it is not possible to conclude from only one test per condition,

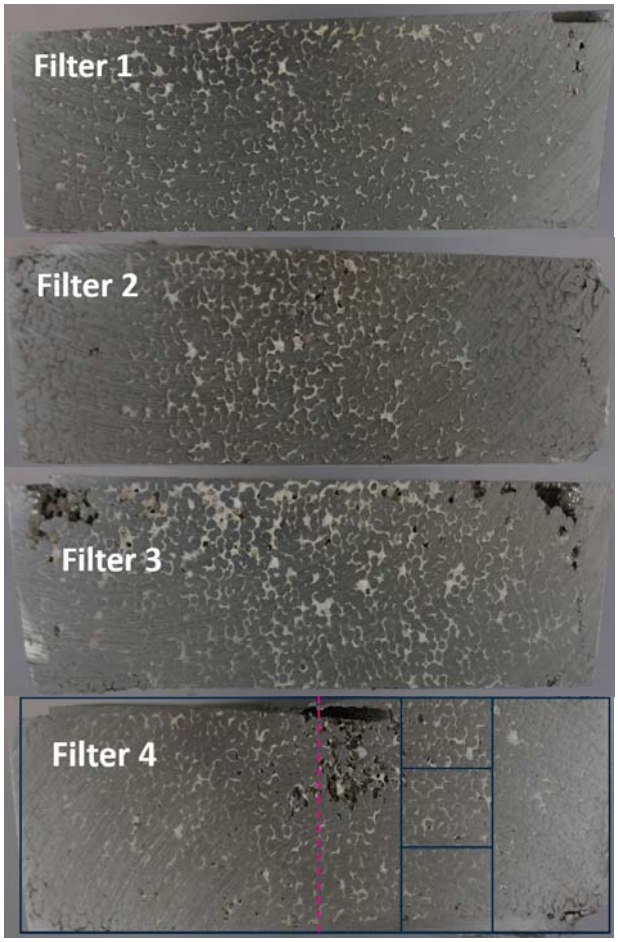

Figure 9 The diagonal cross section of spent filters: filter in white and the metal solidified inside the filter. The width of the filter is 14 cm and the height is 5 cm.

Figure 10 shows the morphology of the solidified melt poured into the filter from the top in test 10. Oxide films from 20 to 80 µm and pores up to 20 µm were observed, in addition to precipitated Al-Fe-Si-Mn on the phase boundary. Oxide film from kitchen foil fold over dry side to dry side during the entrainment [14] into the bulk metal, which formed pores. The action of breaking waves, such as stirring, during the surface folding is potentially the reason for formation of micro-pores, in addition to the magnetic field from the induction furnace.

Spent filters were cut and polished for light microscopic analysis. Figure 11 and Figure 12 show the example of Filters 3 and 4. The sampling position is indicated in the lower left corner of the figure, with the geometry showed in Figure 9. With 10 times magnification, good contact between metal and filter interfaces was observed. Only few inclusions are expected in Filter 3. For Filter 4, large films were collected at the top of the filter and small ones at the bottom area, in addition to the phase boundary. It seems that original oxide films are entangled with each other with a total length up to 1mm.

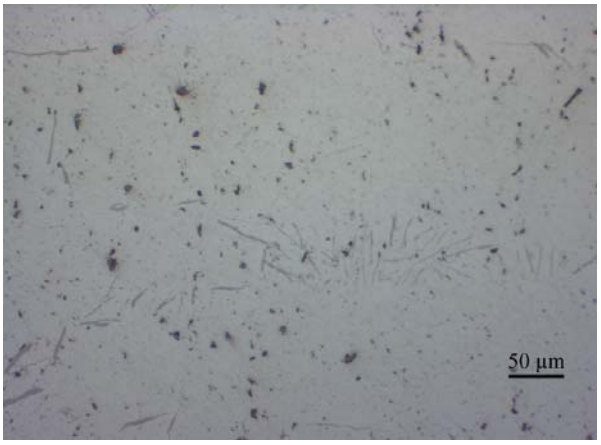

Figure 10 Oxide films and pores in melt before the filter in test 4

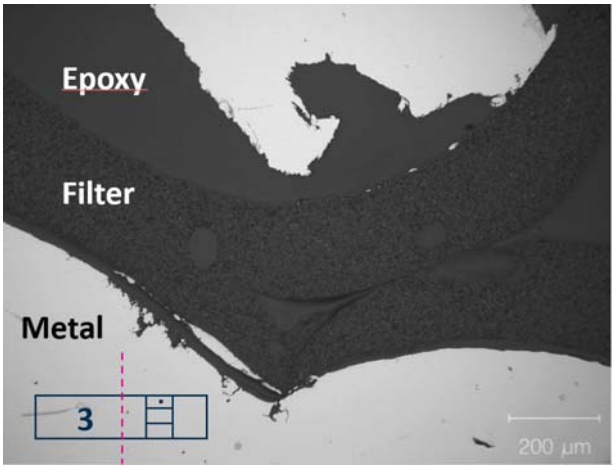

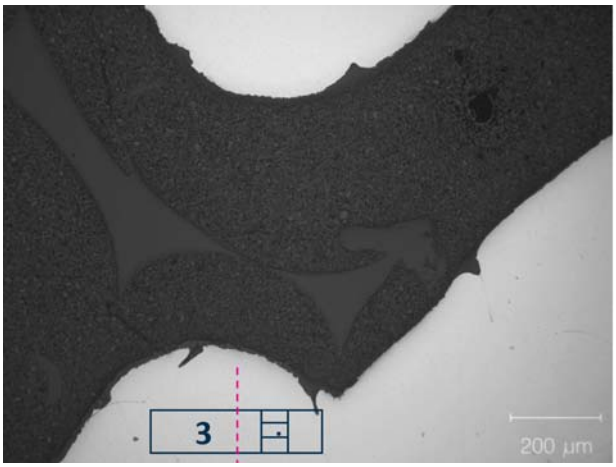

Figure 11 The morphology of the spent filter 9

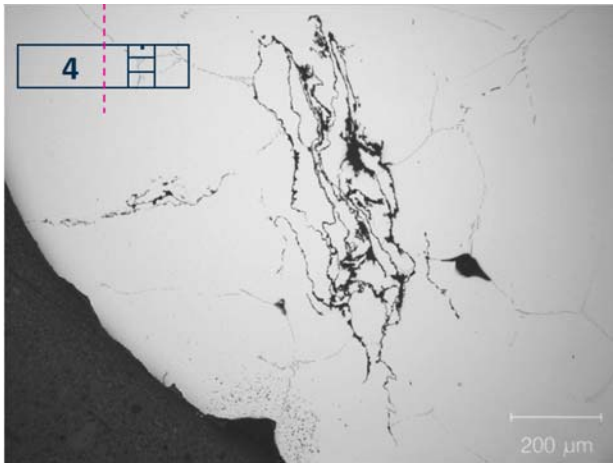

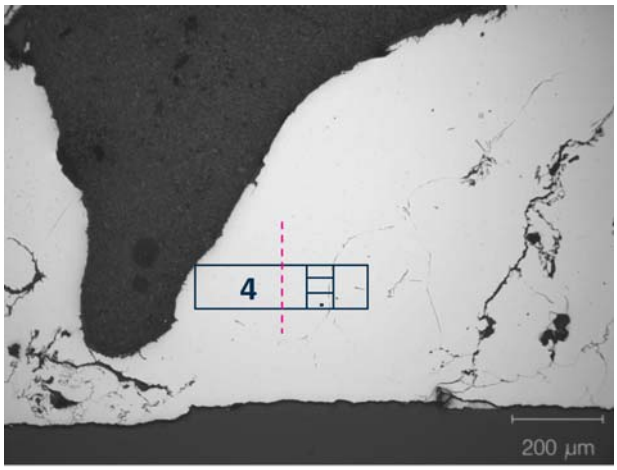

Figure 12 The morphology of the spent filter 4

A 3D micro X-ray computed tomography scan of a sample taken from the top region of filter 4 has been done to verify that the total filter has been properly primed. A cross section is shown in Figure 13. It shows that the filter was properly filled with metal. However, the added films from the aluminium foil are too thin to be detected in the scan with a resolution of 13.6 µm/px.

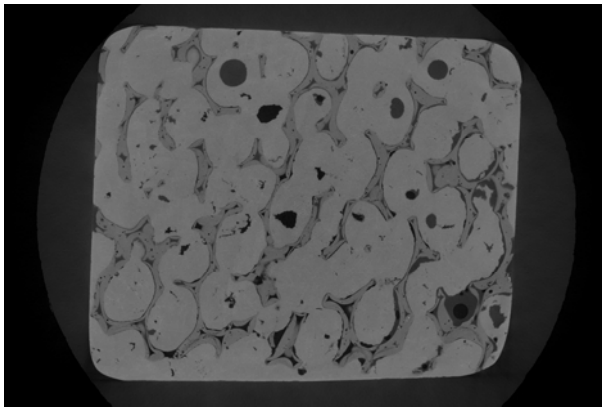

Figure 13: A cross section of a sample from test number 4. The size of the sample is approximately 15×20 mm^2.

Conclusions

In this work, a lab scale experimental set-up was designed and tested with reverse priming of alumina filter. Ar gas pressure drives the upward flow and gravity controls the downward flow. The equipment also offers the possibility of controlling the downward flow with decreasing pressure (this was not done for the present experiments). Good priming for filters 1 (up and down flow), 2 (up and down), 3 (up), and 4 (up and down with added oxide films) is concluded, independently of the flow direction. This is also demonstrated by the morphology of the spent filters. From the present experiments, it was not detected that the filtration behaviour was influenced by reverse priming.

In future tests, particles can be incubated into the filter to study the effect of reverse priming toward inclusion removal. In this case, a traditional gravity filtration test should be carried out for reference.

Acknowledgment

This research was carried out as part of the Norwegian Research Council (NRC) - funded BIA-IPN Project (256724/O20) SmartAl. It includes the following partners: Hydro Aluminium AS, Hydal Aluminium Profiler AS, Hycast AS, Ekornes ASA, NTNU and SINTEF. Funding by the industrial partners and NRC is gratefully acknowledged. Thanks are also given to Arne Nordmark for contributing during the planning phase of the experiments.

References

1. Butcher, K., R. and D. Rogers, B, *Update on the filtration of aluminum alloys with fine pore ceramic foam.* Light Metals 1990: p. 797-803.
2. Alexandre Vianna da Silva, A.M.e.a., *Filtration Efficiency and Melt Cleanness Evaluation using LAIS Sampling at Valesul Aluminio S.A.* Light Metals, 2005: p. 957-960.
3. Instone, S., Badowski, M., Schneider, W et al, *Development of molten metal filtration technology for aluminium.* Light Metals, 2005: p. 933-938.
4. Syvertsen, M., Frisvold, Frede et al, *Development of a compact deep bed filter for aluminum.* Light Metals: Proceedings of Sessions, TMS Annual Meeting (Warrendale, Pennsylvania), 1999: p. 1049-1055.
5. Zhou, M., Shu, D. et al, *Deep filtration of molten aluminum using ceramic foam filters and ceramic particles with active coatings.* Metallurgical and Materials Transactions A (Physical Metallurgy and Materials Science), 2003. **34A**(5): p. 1183-1191.
6. Voigt, C., et al., *Filtration Efficiency of Functionalized Ceramic Foam Filters for Aluminum Melt Filtration.* Metallurgical and Materials Transactions B, 2017. **48**(1): p. 497-505.
7. Fritzsch, R., *Electromagnetically Enhanced Priming of Ceramic Foam Filters.* 2016.
8. Bao, S., et al., *Inclusion (Particle) Removal by Interception and Gravity in Ceramic Foam Filters.* Journal of Materials Science, 2012. **47**(23): p. 7986-7998.
9. Kennedy, M.W., *Removal of Inclusions from liquid Aluminium using Electromagnetically Modified Filtration.* 2013.
10. Eckert, C.E., R.E. Miller, and D. Alelian, *Molten aluminum filtration: fundametals and models.* Light Metals, 1984: p. 1281-1304.
11. Tundal, U., Steen,.I.K., *Apparatus and Method for The Removal of Unwanted Inclusions from Metal Melts*. WO 2016/126165 A1.
12. Moeland, G., E. Myrbostad, and K. Venas. *Hycast I-60 SIR-a new generation inline melt refining system*. in *LIGHT METALS-WARRENDALE-PROCEEDINGS-*. 2002. TMS.
13. Wang, D.-J. and S.-T. Wu, *The influence of oxidation on the wettability of aluminum on sapphire.* Acta metallurgica et materialia, 1994. **42**(12): p. 4029-4034.
14. Campbell, J., *Castings*. 2003: Elsevier Science.